Universal Stability Properties for Multi-Layer Hele-Shaw Flows and its Application to Instability Control

Prabir Daripa[1,*] and Xueru Ding [2]

[1]Department of Mathematics, Texas A&M University, College Station, TX-77843

[2]Department of Petroleum Engineering, Texas A&M University at Qatar, Doha, Qatar

December 26, 2011

Abstract

With the motivation of understanding the effect of various injection policies currently in practice for chemical enhanced oil recovery, we study linear stability of displacement processes in a Hele-Shaw cell involving injection of an arbitrary number of fluid phases in succession. This work mainly builds upon our earlier study for the three-layer case [P. Daripa, Studies on stability in three-layer Hele-Shaw flows, *Physics of Fluids*, (20), 2008]. Stability results obtained for an arbitrary number of displacing fluids in succession reduce to Saffman-Taylor case when there is only one displacing fluid. The stability results have been applied here to design injection policies that are considerably less unstable than the pure Saffman-Taylor case. Implementation of such injection policies based on the application of the stability results is likely to improve oil recovery.

Keywords: Hydrodynamic Stability, Saffman-Taylor Instability, Linear Stability, Chemical Enhanced Oil Recovery

_____

*Author for correspondence (e-mail: prabir.daripa@math.tamu.edu)

1 Introduction

The displacement of a more viscous fluid by a less viscous one is known to be potentially unstable in a Hele-Shaw cell. Such flows first studied by Hele-Shaw [14] are known as Hele-Shaw flows and have similarities with porous media flows [2] in the sense that in both of these flows, fluid velocity is proportional to the pressure gradient. Because of this analogy and relative ease and accuracy with which such Hele-Shaw flows can be experimentally studied in comparison to flows in porous media, Hele-Shaw flows have been studied extensively over many decades. The instability theory in this context, also known as Saffman-Taylor instability [23], is now well developed for single-interface flows. Exact growth rates of interfacial disturbances for such flows are well known and well-documented in standard textbooks on hydrodynamic stability theory, e.g. Drazin & Reid [10].

Exact known stability results from these past works (see also formulas (1) and (2)) imply that increasing the interfacial tension suppresses instability whereas increasing the positive viscosity-jump at the interface in the direction of flow further enforces instability ([10]). Based on this understanding, it is a common practice to use a layer of third fluid in between having viscosity less than that of the displaced fluid and more than that of the displacing fluid, in the hope that it will suppress the growth of instability that is otherwise present in the absence of this middle layer ([25], [28], [24]). This expectation is justified based on the application of our understanding of single-interface flows to multi-interface case under the assumptions that (i) effect of interfacial interactions is negligible, and (ii) interfacial tensions at two interfaces are similar to the interfacial tension at the original interface between the displaced and the displacing fluid in the absence of the middle-layer. This makes each of these interfaces less unstable individually due to reduction in viscosity-jump across them. However, when interfacial tensions as well as the viscosity-jumps at two interfaces are significantly modified due to the middle layer fluid, it is not easy to correctly predict the outcome of these collective effects on the overall instability of these flows from simple extrapolation of our understanding of single-interface flows. This problem becomes even more daunting in the case of flows with an arbitrary number of interfaces.

Such flows involving arbitrary number of interfaces arise during various flooding schemes in chemical enhanced oil recovery, a subject of intense current interest due to rising energy demand world wide in a market of tight supply. To alleviate this situation, there is an ongoing much needed research in the energy resources area. One such energy resources area is oil recovery. A fractional increase in rate of oil recovery from an oil field using new oil recovery technology or even smarter use of existing technology will have a lot of impact worldwide. Economic and geological uncertainty play a critical role in deciding the producing life of an oil field. Although there may still be producible oil in a field, economics of water handling and geological uncertainty of permeability fields and to a lesser extent porosity fields make producing the remaining oil economically very arduous. Currently, early water breakthroughs (which exacerbate the economics) limit oil recovery ranging from 10% to 35% depending on the type of reservoir. Typically, after primary production a waterflood is employed for pressure support and to further sweep any oil that is left over, thus decreasing the field oil saturation. One potential drawback, though, for the waterflood is the inability to accurately sweep the oil due to an inadequate mobility ratio. Because of this drawback, it is estimated that total residual oil in matured reservoirs (reservoirs after conventional primary and secondary oil recovery) around the world is around 70% of the original oil in place (OOIP). Therefore, it is important to investigate other alternatives to a waterflood.

These alternative methods are called Enhanced Oil Recovery (EOR) methods. One such EOR method

is the surfactant flood. Surfactants are effective in lowering the interfacial tension between oil and water to a level that promotes mobilization of trapped oil drops (see Shah and Schecter [24]). Surfactant floods (see Fathi et.al. [11]) have been used for EOR and lessons learned from this has been applied for aquifer remediation (see Pope [21]). Another such method is polymer flooding. Polymer floods differ from water floods in that polymer floods rely on reducing mobility contrast between displacing and displaced fluids. Polymer-flooding was attempted in early seventies. The idea of using polymer-flooding to improve oil recovery started evolving through the seventies which is well documented in various conference proceedings, books, and journal articles of the seventies ([9, 12, 15, 17, 20, 22, 24, 28]). In early eighties, this polymer-flooding process was mathematically formulated and solved numerically by Daripa et.al. [5]. In most field tests with this flooding process, recovery was less than 10%. It was felt that this failure is perhaps due to (i) a loss of polymer in the rock matrix of porous media, (ii) polymer degradation, and (iii) a lack of understanding of some fundamental issues of this technology such as timing of the start of this flood in relation to the water flood that should precede this polymer-flooding process. Before a systematic study could be undertaken to get to the bottom of all sources of this failure and thereby improve the polymer-flooding strategy, interest in this polymer-flooding process waned significantly in most countries except in China, partly due to low labor cost. Corlay and Delamaide [1] presents whole history of the Daqing polymer-flooding project. The Daqing field is the largest oil field in the People's Republic of China with original oil in place exceeding two billion tons.

Combining the above two methods into one that simultaneously reduces capillary pressure as well as reduces the mobility contrast is a better alternative perhaps. This alternative technology is called ASP (Alkaline-Surfactant-Polymer) flooding which also helps in addressing challenges to recover oil from subsea, deep-sea reservoirs and also from the formations where the mobility of the in-situ oil being recovered is significantly less than that of the drive fluid used to displace the oil. The alkaline in ASP is used so that it reacts with the acid components of crude oil and generate in situ surfactant which overcomes the surfactant depletion in the liquid phases due to retention by the rock matrix. ASP-flooding for EOR is relatively new and is being evaluated through laboratory investigations as well as field tests in many places. Successful results on ASP pilot tests in Cambridge [29], in Daqing and Gudong oil fields in China [8, 31] and many other oil fields around the globe including Venezuela [30] have generated intense interest in ASP-flooding [31]. Books by Littman [16] and Sorbie [26] and most recent article by Needham and Doe [18], Zhijun and Yongmei [32], and Taylor and Nasr-El-Din [27] make the case, through all kinds of review, for ASP usage to improve oil recovery. Field tests are encouraging (recoveries are 25-30%) but at this recovery rate, economics are marginal at best. Investment in the basic research of this EOR method by ASP-flooding (Polymer flooding is a special case of ASP-flooding) will ensure that this method has an important place in oil production for a long time to come.

Many of the modern EOR chemical flooding schemes use injection of a sequence of simple to such complex fluids in succession with the hope of suppressing fingering instability and reducing capillary pressure, thereby improving oil recovery. All these injection policies involve motion of arbitrary number of sweeping interfaces. Unfortunately, even the basic stability results for flows involving motion of multiple interfaces which can be helpful in the smart design of such flooding schemes are not available. An attempt to address these challenges has been made in recent years by undertaking systematic linear stability studies of multi-layer Hele-Shaw flows. Review of some of the key results known in this area will now be presented in the next section. Careful reading of the next review section is essential to apprehend the significance of the universal

3

results to be presented in section 4. Next section is then followed by section 3 on Mathematical Formulation. Sections 4 and 6 are about universal stability properties related to dispersion curves, unstable waves, and neutral waves of multi-layer Hele-Shaw flows. Numerical results and the use of universal stability properties for the design of smart multi-layer injection policies are presented in sections 5 and 7. Finally, we conclude in section 8.

2   Preliminaries

Two-layer Hele-Shaw flows in which a fluid is displacing another fluid of higher viscosity with both fluid layers extending up to infinity away from the common interface is the most celebrated case in the context of linear instability of the interface separating these two fluids. If μ_r is the viscosity of the displaced fluid, μ_l ($\mu_l < \mu_r$) is the viscosity of the displacing fluid, U is the constant velocity of the rectilinear flow, and the interfacial tension at the interface is constant T, then the growth rate σ_{st} of the interfacial disturbance having wave-number k is given by

$$\sigma_{\mathrm{st}}(k) = \frac{Uk(\mu_r - \mu_l) - k^3 T}{\mu_r + \mu_l}, \tag{1}$$

from which it follows that the maximum growth rate σ_{sm} and corresponding dangerous wavenumber k_{sm} are given by

$$\sigma_{\mathrm{sm}} = \frac{2T}{(\mu_r + \mu_l)} \left(\frac{U(\mu_r - \mu_l)}{3T} \right)^{3/2}, \qquad k_{\mathrm{sm}} = \sqrt{\frac{U}{3T}(\mu_r - \mu_l)} \tag{2}$$

The critical (also known as cut-off) wave number for which the wave is neutral (i.e., growth rate zero) is given by

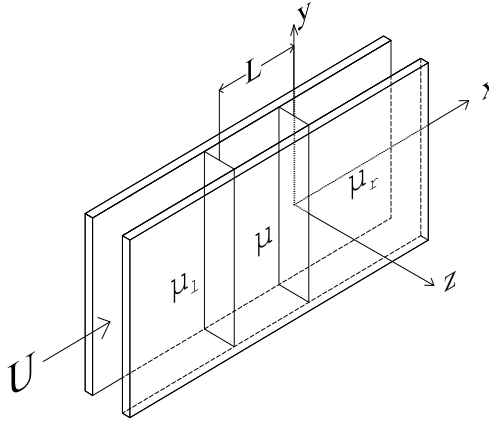$$k_{cr} = \sqrt{\frac{U}{T}(\mu_r - \mu_l)}. \tag{3}$$

Figure 1: Three-layer fluid flow in a Hele-Shaw cell

The three-layer Hele-Shaw flow is an extension of this two-layer single-interface Hele-Shaw flow. The set-up is shown in Fig. 1. The fluid upstream (i.e., as $x \to -\infty$) has a velocity $\mathbf{u} = (U, 0)$. The fluid in the extreme left layer with viscosity μ_l extends up to $x = -\infty$, the fluid in the extreme right layer with viscosity $\mu_r > \mu_l$ extends up to $x = \infty$, and the fluid in-between middle-layer with constant viscosity μ_1

$(\mu_r > \mu_1 > \mu_l)$ is of finite extent of length L. Thus, this is a flow with two interfaces. Let T_0 and T_1 be the interfacial tensions of the leading and the trailing interfaces respectively. Some facts about this problem from Daripa [4] will now be mentioned. There are two modes (eigenvalues) denoted by σ_+ and σ_- for each wave and corresponding dispersion relations $\sigma_+(k)$ and $\sigma_-(k)$ do not have explicit forms such as (1) for the two-layer case. However, these can omputed. Plots of these dispersion relations can be found in Daripa [4]. Exact formulas similar to (2) for the maximum growth rate and the most dangerous wavenumber are not available. However, an explicit formula for an upper bound on the maximum growth rate is given by (from Daripa [4])

$$\sigma < \sigma_u = \max\left\{\frac{2T_0}{\mu_r}\left(\frac{U(\mu_r - \mu_1)}{3T_0}\right)^{3/2}, \frac{2T_1}{\mu_l}\left(\frac{U(\mu_1 - \mu_l)}{3T_1}\right)^{3/2}\right\}, \tag{4}$$

and the cutoff wave numbers k_1 and k_2 of $\sigma_+(k)$ and $\sigma_-(k)$ respectively are given by

$$k_1 = \sqrt{\frac{U}{T_0}(\mu_r - \mu_1)} \quad \text{and} \quad k_2 = \sqrt{\frac{U}{T_1}(\mu_1 - \mu_l)}. \tag{5}$$

The necessary condition for a mode with wavenumber k to be unstable is $k \le \max(k_1, k_2)$ and a sufficient condition is $k \le \min(k_1, k_2)$. The two cut-off wavenumbers k_1 and k_2 become equal, called critical wave number and denoted by k_{cr}, when the middle layer viscosity μ_1 takes a specific value, called critical viscosity and denoted by μ_{cr}. These critical values are given by

$$\mu_{cr} = \mu_r - \frac{T_0}{T_0 + T_1}(\mu_r - \mu_l), \qquad k_{cr} = \sqrt{\frac{U}{T_0 + T_1}(\mu_r - \mu_l)}. \tag{6}$$

All waves in the range $0 < k < k_{cr}$ are unstable when middle layer viscosity $\mu_1 = \mu_{cr}$. The k_{cr} is the shortest
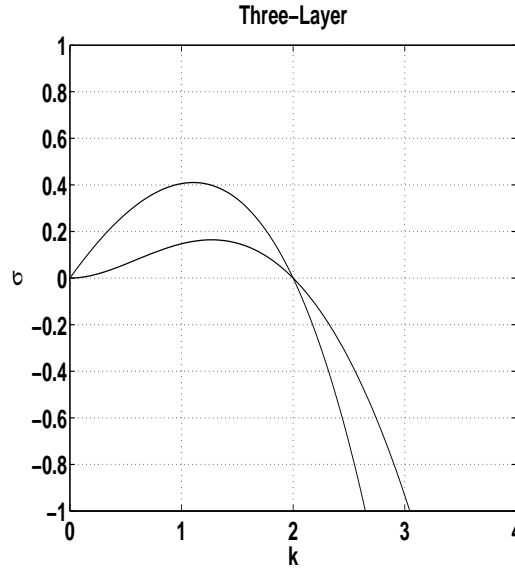

Figure 2: Plots of dispersion curves $\sigma_-(k)$ and $\sigma_+(k) > \sigma_-(k)$ for the three-layer case when $\mu_1 = \mu_{cr}$. The parameter values used for these plots are $\mu_l = 2, \mu_1 = 6, \mu_r = 10, T_0 = T_1 = U = 1$ and $L = 1$. The viscosity $\mu_1 = 6$ is the critical viscosity μ_{rmcr} given by formula (6).

unstable bandwidth k_{cr}. In general for other values of μ_1, the unstable bandwidth is $\max(k_1, k_2)$ when at least one of modes is positive. Figure 2 shows the plots of the two dispersion curves when the middle layer

viscosity $\mu_1 = \mu_{\mathrm{cr}}$ with the other parameter values $\mu_l = 2$, $\mu_r = 10$, $T_0 = T_1 = 1$, $U = 1$ and $L = 1$. We see that $\sigma_+ = \sigma_- = 0$ at $k = k_{\mathrm{cr}}$ as it should be.

In closing this section, there are several observations to be made here for the three-layer case. It will be helpful in conclusion to see the generalization of these to multi-layer case and much more.

1. Notice the similarity between the formula (2) for the maximum growth rate σ_{sm} for the two-layer case and the formula (4) for the upper bound σ_{u} on the same for the three-layer case. In the three-layer case, the strict upper bound σ_{u} is the maximum of the modified maximum individual Saffman-Taylor growth rates of two interfaces. This formula does not depend on L. However, the maximum growth rate depends on L (see Daripa [4]).

2. The cut-off wavenumbers k_1 and k_2 given by (5) are same as the individual cut-off wave numbers for the two interfaces that one obtains from applying the pure Safmman-Taylor formula (3) to two individual interfaces with correct values of the viscosity across the interfaces used in this formula. Important thing to notice is that formulas (5) for k_1 and k_2 do not depend on the length, L, of the middle layer.

3. Notice that μ_{cr} and k_{cr} given by (6) do not depend on the length L of the middle layer. Since individual growth rates of the two interfaces are given by the Saffman-Taylor formulae in the limit $L \to \infty$, one can easily verify that individual Saffman-Taylor growth rate of each of the two interfaces are zero at $k = k_{\mathrm{cr}}$ provided $\mu_1 = \mu_{\mathrm{cr}}$.

4. Notice the similarity between the formula (3) for the critical (same as cut-off) wavenumber in the two-layer case and the formula $(6)_2$ for the same in the three-layer case. These two formulas, in fact, can be unified into one as

$$k_{\mathrm{cr}} = \sqrt{\frac{U}{T_{\mathrm{total}}}(\mu_r - \mu_l)}, \tag{7}$$

with T_{total} in the formula standing for the sum of the interfacial tensions of all interfaces. For the pure Saffman-Taylor case, there is only one mode and hence only one cut-off wavenumber. In this case, the cut-off wavenumber is also called critical wavenumber, though this is not the case for the three-layer flows. For three-layer flows, there are two modes and thus two distinct cutoff wavenumbers k_1 and k_2 (see formula (5)) in general unless they become same $k_1 = k_2 = k_{\mathrm{cr}}$ when $\mu_1 = \mu_{\mathrm{cr}}$ which (see formulas $(6)_1$) if written in terms of T_{total} becomes

$$\mu_{\mathrm{cr}} = \mu_r - \frac{T_0}{T_{\mathrm{total}}}(\mu_r - \mu_l). \tag{8}$$

5. In the section 4, we will see that for the three-layer case there is another choice for the (critical) viscosity of the middle layer, namely $\sqrt{\mu_r \mu_l}$, when the unstable bandwidth will also be shortest as given by (7) provided the interfacial surface tensions are chosen carefully (special case of (34) with $N = 1$).

In this paper, we show not only the generalization of the above results to multi-layer Hele-Shaw flows but also discover new results even for the special case of three-layer flows. Results related to upper bounds on the maximum growth rate for the multi-layer Hele-Shaw flows are available from Daripa ([3]. These results will be briefly mentioned in the section 8 on conclusions. Next we briefly present the mathematical formulation and the numerical scheme to solve for the dispersion relations and obtain other analytical relations.

3 Mathematical formulation

The physical set-up consists of rectilinear motion in a Hele-Shaw cell of many immiscible fluids having different viscosity from each other. The physical set-up for the special case when there are only three fluids is shown in Fig. 1. This case is the building block for flows involving more than three fluids such as the one sketched in Fig. 3 involving $N + 1$ number of interfaces with N number of interior layers.

The flow domain is $\Omega := (x, y) = \mathbb{R}^2$ (with a periodic extension of the set-up in the $y-$direction). The fluid upstream (i.e., as $x \to -\infty$) has a velocity $\mathbf{u} = (U, 0)$ and constant viscosity μ_l which occupies the region $x < -L$ in the moving frame (moving with velocity $(U, 0)$). Similarly, the fluid in the region $x > 0$ in the moving frame has viscosity μ_r. There are N interior regions of the equal length L/N in the interval $(-L, 0)$ (see Fig. 3). Each of these regions contains constant viscosity fluids μ_i, $i = 1, 2, ..., N$ such that viscosity increases in the direction of basic flow, i.e., $\mu_r > \mu_1 > \mu_2 > \mu_3 .... > \mu_N > \mu_l$. Thus, this set-up has $(N + 1)$ interfaces located at $x = 0, -L/N, ..., -L$ with corresponding interfacial tension coefficients denoted by T_i, $i = 0, 1, ..., N$.
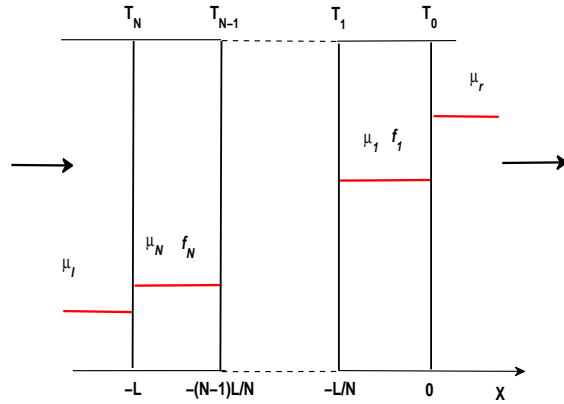

Figure 3: Multi-layer fluid flow

The fluid flow in each layer is described by the governing equations

$$\nabla \cdot \mathbf{u} = 0, \quad \nabla p = -\mu \, \mathbf{u}, \quad \frac{D\mu}{Dt} = 0, \tag{9}$$

where $\nabla = \left(\frac{\partial}{\partial x}, \frac{\partial}{\partial y} \right)$ and $\frac{D}{Dt}$ is the material derivative. The first equation $(9)_1$ is the continuity equation for incompressible flow, the second equation $(9)_2$ is the Darcy's law (Darcy [2]), and the third equation $(9)_3$ is the advection equation for viscosity (Gorell & Homsy [13], Daripa & Pasa [7]). This last equation simply states that the viscosity is a property of the fluid and thus gets advected by the fluid. Below, we refer this model as the Hele-Shaw model (see also Daripa et. al. ([3], [4]). Gorell and Homsy [13], & Pearson [19]).

The above system (9) admits a simple basic solution, namely the whole fluid set-up moves with velocity $(U, 0)$ with all its interfaces being planar, i.e. parallel to the y-axis. The pressure corresponding to this basic solution is obtained by integrating $(9)_2$. In a frame moving with velocity $(U, 0)$, the above system consisting

7

of all planar interfaces and all fluid layers is stationary . Here and below, with slight abuse of notation, the same variable x is used in the moving reference frame. In linearized stability analysis by normal modes, disturbances (denoted by tilde variables below) in the moving reference frame are written in the form

$$(\widetilde{u}, \widetilde{v}, \widetilde{p}, \widetilde{\mu}) = (f(x), \psi(x), \phi(x), h(x))e^{(iky+\sigma t)} \tag{10}$$

where k is the wave number and σ is the growth rate. We then insert this disturbance form into the linearized disturbance equations obtained from (9) and also into the linearized dynamic and kinematic interfacial conditions. The details of these calculations when there is only one interior interface can be found in Daripa and Pasa [6]. Thus, we obtain the following system of N equations, one for each interior region.

$$f_{i_{xx}} - k^2 f_i = 0, \quad (i = 1, ..., N) \tag{11}$$

These equations also hold in the two exterior regions whose solutions due to exponential decay of eigenfunction in the far field are given by $f(x) = f(0)\exp(-x)$, $x > 0$ and $f(x) = f(-L)\exp(x)$, $x < -L$. Similarly, the interfacial conditions at $N+1$ interfaces are written down easily from extending single interface results (see Daripa and Pasa [6]).

$$- \mu_1 f_{1_x}^-(0) = (\mu_r k - \lambda E_0)f_1(0) \tag{12}$$

$$\mu_i f_{i_x}^+(-iL/N) - \mu_{i+1} f_{i+1_x}^-(-iL/N) = -\lambda E_i f_i(-iL/N), \quad i \in [1, N-1] \tag{13}$$

$$\mu_N f_{N_x}^+(-NL/N) = (\mu_l k - \lambda E_N)f_N(-NL/N), \tag{14}$$

Above we have used $\mu_0 = \mu_r, \mu_{N+1} = \mu_l$ and

$$E_i = k^2 U(\mu_i - \mu_{i+1}) - T_i k^4, \quad i = 0, 1, \dots, N. \tag{15}$$

The continuity of eigenfunctions (i.e. $f_0(0) = f_1(0)$ and $f_N(-L) = f_{N+1}(-L)$) at the exterior interfaces have already been used in deriving (12) and (14) above. The similar conditions at $(N-1)$ interior interfaces give

$$f_i(-iL/N) = f_{i+1}(-iL/N) \quad (i = 1, ..., N-1). \tag{16}$$

The general solution of equation (11) is $f_i(x) = C_i \, exp(-kx) + D_i \, exp(kx)$ for each interior domain $-iL/N < x < -(i-1)L/N$, $i = 1, 2, ...N$. Substituting the solution into the boundary conditions (12) and (16) leads to a matrix equation $AX = 0$ for the unknown constant vector $X = (C_1, D_1, ..., C_N, D_N)$. The matrix A is a square matrix $(2N \times 2N)$, whose entries are denoted by A_{ij}, $i, j = 1, 2, \cdots, 2N$,

$$A = \begin{vmatrix} A_{11} & A_{12} & 0 & 0 & 0 & \cdots & 0 \\ A_{21} & A_{22} & A_{23} & A_{24} & 0 & \cdots & 0 \\ A_{31} & A_{32} & A_{33} & A_{34} & 0 & \cdots & 0 \\ & & & \cdots\cdots & & & \\ 0 & \cdots & 0 & A_{2N-2,2N-3} & A_{2N-2,2N-2} & A_{2N-2,2N-1} & A_{2N-2,2N} \\ 0 & \cdots & 0 & A_{2N-1,2N-3} & A_{2N-1,2N-2} & A_{2N-1,2N-1} & A_{2N-1,2N} \\ 0 & \cdots & 0 & 0 & 0 & A_{2N,2N-1} & A_{2N,2N} \end{vmatrix}.$$

As an example, for the case of three intermediate layers A_{ij} are given by

$$A_{11} = \sigma(\mu_1 - \mu_r)k + E_0, \quad A_{12} = -\sigma(\mu_1 + \mu_r)k + E_0,$$
$$A_{21} = (-\sigma\mu_1 k + E_1)e^{(kL/N)}, A_{22} = (\sigma\mu_1 k + E_1)e^{(-kL/N)},$$
$$A_{23} = \sigma\mu_2 ke^{(kL/N)}, A_{24} = \sigma\mu_2 ke^{(kL/N)},$$
$$A_{31} = -e^{(kL/N)}, A_{32} = e^{(-kL/N)}, A_{33} = e^{(kL/N)}, A_{34} = -e^{(-kL/N)},$$
$$A_{43} = (-\sigma\mu_2 k + E_2)e^{(2kL/N)}, A_{44} = (\sigma\mu_2 k + E_2)e^{(-2kL/N)},$$
$$A_{45} = \sigma\mu_3 ke^{(2kL/N)}, A_{46} = -\sigma\mu_3 ke^{(-2kL/N)},$$
$$A_{53} = -e^{(2kL/N)}, A_{54} = e^{(-2kL/N)}, A_{55} = e^{(2kL/N)}, A_{56} = -e^{(-2kL/N)},$$
$$A_{65} = (\sigma(\mu_4 + \mu_l)k - E_3)e^{(3kL/N)}, A_{66} = (\sigma(-\mu_4 + \mu_l)k - E_3)e^{(-3kL/N)}.$$

The first line of matrix A comes from the boundary condition in equation (12), the second and fourth lines are from the boundary condition in equation (13), the third and fifth lines are from the boundary condition in equation (16), and the last line is from the boundary condition in equation (14). We notice that in this example, there are no σ term in the third and fifth lines. We then conclude that there are no σ in $(N-1)$ rows of $(2N \times 2N)$ matrix A. The solvability condition, namely the determinant of matrix $\det(A) = 0$ for a nontrivial solution, leads to the dispersion relation. Since the highest degree of $\det(A) = 0$ is $(N+1)$, there will be $(N+1)$ roots corresponding to $(N+1)$ interfaces. These roots are found numerically to obtain the dispersion relations. These numerically obtained dispersion relations will be plotted in sections below as necessary.

4   Universal Stability Properties

The dispersion curves $\{\sigma_i(k), i = 0, ..., N\}$ are computed for some choices of N by solving the $(N+1)$ degree polynomial resulting from the solvability condition $\det(A) = 0$. These curves are shown later. First we derive some exact results from analyzing this solvability condition. We notice from the form of the matrix A and its entries in the previous section that if $E_i = 0$ for any one of $i = 0, 1, ..., N$, then $\det(A)$ will be of the following form:

$$det(A) = \sigma(k)a(\sigma(k)), \tag{17}$$

where $a(\sigma(k))$ is a function of σ and k. Since $E_i = k^2 U(\mu_i - \mu_{i+1}) - T_i k^4 = 0$ at $k = k_i \equiv \sqrt{U(\mu_i - \mu_{i+1})/T_i}$, it follows from the solvability condition $det(A) = 0$ and equation (17) that there is one mode $\sigma_i(k) = 0$ at $k = k_i$. In general, each of the modes $\sigma_i(k) = 0$ at a wave number k_i distinct from the other ones and thus we have

$$k_i = \sqrt{\frac{U(\mu_i - \mu_{i+1})}{T_i}}, \quad i = 0, 1, ... N. \tag{18}$$

These are the cut-off wavenumbers for the $(N+1)$ dispersion curves. Notice that these cut-off wave numbers do not depend on L and thus, not surprisingly, correspond to cutoff wave numbers for dispersion curves of $N+1$ individual interfaces determined simply by applying pure Saffman-Taylor formula (3) to all these individual interfaces with correct values of the viscosity across the interfaces used in this formula. If we define

$$k_{\max} = \max(k_0, k_1, \cdots, k_N), \quad \text{and} \quad k_{\min} = \min(k_0, k_1, \cdots, k_N), \tag{19}$$

9

then it is obvious that at least one of the modes is positive if wave-number k satisfies

$$k \leq k_{\max}. \tag{20}$$

and all modes are positive for a wave satisfying

$$k \leq k_{\min}. \tag{21}$$

Thus inequality (20) is a necessary condition for instability of a mode with wavenumber k whereas inequality (21) is a sufficient condition for instability of a mode with wavenumber k. Notice that $k_{\max}$ and $k_{\min}$ are both L-independent.

Moreover, when $E_0 = ... = E_N = 0$ at the wave number $k = k_{cr}$, that means $k_0 = ... = k_N = k_{cr}$. In this case, determinant of matrix A has the following form (see the matrix A and its entries in the previous section):

$$det(A) = b(k_{cr})\sigma^{N+1}, \tag{22}$$

where $b(k_{cr})$ is a function of k_{cr}. It is easy to see that the $(N+1)$ roots of equation (22) are all zero, that is

$$\sigma_i = 0, \qquad i = 0, 1, ...N. \tag{23}$$

We can solve for k_{cr} and the "critical" viscosities $\mu_{cr}^{(i)}, i = 1, ...N$ for the N layers from $(N+1)$ equations $E_i = 0, \quad i = 0, 1, ...N$, or equivalently from

$$\left.\begin{array}{l} k_{cr}^2 U(\mu_r - \mu_1) - T_0 k_{cr}^4 = 0, \\ k_{cr}^2 U(\mu_1 - \mu_2) - T_1 k_{cr}^4 = 0, \\ \cdots \cdots \\ k_{cr}^2 U(\mu_N - \mu_l) - T_N k_{cr}^4 = 0. \end{array}\right\} \tag{24}$$

By adding all the above equations together, we solve for k_{cr} in terms of viscosities of extreme layers which is given below. Then substituting the formula of k_{cr} in each of the above equations, we obtain the following formulas for the N critical viscosities $\mu_{cr}^{(1)}, ..., \mu_{cr}^{(N)}$.

$$\left.\begin{array}{l} k_{cr} = \sqrt{\frac{U(\mu_r - \mu_l)}{T_{\text{total}}}}, \\ \mu_{cr}^{(1)} = \mu_r - \frac{T_0}{T_{\text{total}}}(\mu_r - \mu_l), \\ \mu_{cr}^{(2)} = \mu_{cr}^{(1)} - \frac{T_1}{T_{\text{total}}}(\mu_r - \mu_l), \\ \cdots \cdots \\ \mu_{cr}^{(N-1)} = \mu_{cr}^{(N-2)} - \frac{T_{N-2}}{T_{\text{total}}}(\mu_r - \mu_l), \\ \mu_{cr}^{(N)} = \mu_{cr}^{(N-1)} - \frac{T_{N-1}}{T_{\text{total}}}(\mu_r - \mu_l), \end{array}\right\} \tag{25}$$

where $T_{\text{total}} = (T_0 + T_1 + \cdots + T_N)$ is the sum of interfacial tensions of all $(N+1)$ interfaces. It is easy to verify that all the above results when $N = 1$ are in agreement with the results for the three-layer case given in section 2.

In general, all waves satisfying $k < k_{\max}$ (see equation $(19)_1$) are unstable since at least one of the modes is always positive in this range. However, when fluids in N layers have critical viscosities μ_{cr} according to the formulas given above, the unstable bandwidth is given by k_{cr}. We claim that this is the shortest bandwidth

for unstable waves meaning $k_{cr} \leq k_{max}$, similar to the three-layer case. We show this next. We recall the following inequality

$$\frac{\sum_i^n P_i}{\sum_i^n Q_i} \leq \max_i \frac{P_i}{Q_i}, \tag{26}$$

which holds for arbitrary n under the condition $P_i > 0$, $Q_i > 0$ ($i = 1, ..., n$). Using this inequality with $P_i = U(\mu_i - \mu_{i+1}), Q_i = T_i$, we obtain

$$\frac{U(\mu_r - \mu_1) + U(\mu_1 - \mu_2) + ... + U(\mu_{N+1} - \mu_l)}{T_0 + T_2 + ... + T_N} \leq \max_i \frac{U(\mu_i - \mu_{i+1})}{T_i} \tag{27}$$

or equivalently,

$$\frac{U(\mu_r - \mu_l)}{T_{\text{total}}} \leq k_{max}^2, \tag{28}$$

where we have used the definition $(19)_1$ for k_{max}. Since the left side of inequality (28) is k_{cr}^2, it follows that $k_{cr} \leq k_{max}$, a generalization of the same result from the three-layer case. ∎
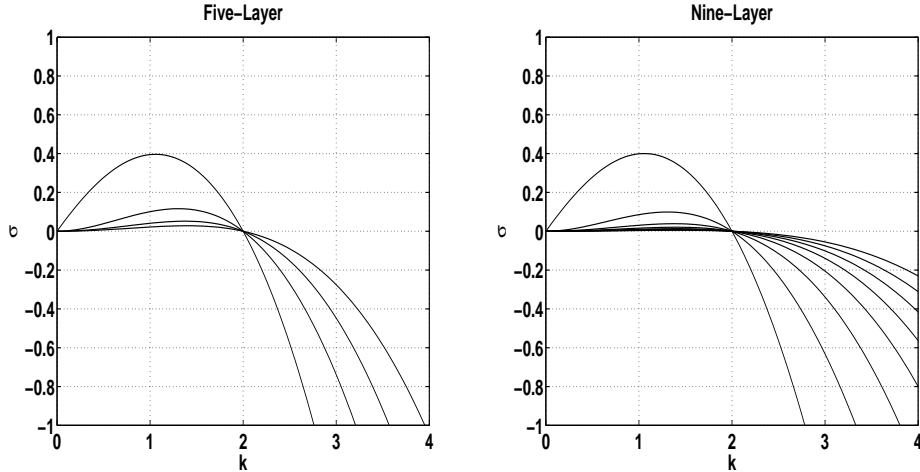

Figure 4: Dispersion relations: growth rates versus wave number k. Five-layer parameter values are: viscosity $\mu = (2, 4, 6, 8, 10)$, $N = 3$, $T_0 = ... = T_3 = 1/2$, $U = 1$ and $L = 1$. Nine-layer parameter values are: viscosity $\mu = (2, 3, 4, 5, 6, 7, 8, 9, 10)$, $N = 7$, $T_0 = ... = T_7 = 1/4$, $U = 1$ and $L = 1$.

5 Numerical Results

It is interesting to observe that the shortest bandwidth k_{cr} is only dependent on U, $(\mu_r - \mu_l)$ and T_{total}. This means that the critical wave number k_{cr} will remain same for arbitrary number of internal layers, N, provided U, $(\mu_r - \mu_l)$ and T_{total} are kept fixed regardless of individual non-zero interfacial tension values of $N + 1$ interfaces and the internal N layers fluid viscosities are $\mu_{cr}^{(i)}, i = 1, ..., N$ given by (25). Figure 4 shows the dispersion plots for five-layer, and nine-layer Hele-Shaw flows respectively with the same value for U, same total interfacial tension T_{total}, and same viscosity difference $(\mu_r - \mu_l)$ between two extreme-layer fluids. Notice that all modes have value zero at the same wave number $k = k_{cr}$ as it should be.

Pure Saffman-Taylor case is a special case of multi-layer case when $N = 0$ corresponding to no internal layer (layer of finite thickness). From enhanced oil recovery perspective, one of the reasons to have several layers with constant viscosity of each layer increasing in the direction of basic velocity U is obviously to stabilize the system i.e., to have $\sigma_{\max}$ of the multi-layer system lower than the pure Saffman-Taylor growth rate σ_{sm}. Notice that we used the words "stabilize the system" here and below to mean "to make the system less unstable". In Daripa [3], a family of upper bounds for the maximum growth rate for multi-layer system has been presented one of which is the extension of the formulae (4) from three-layer to multi-layer. In general, for multi-layer case with appropriate choices of interfacial tensions and the intermediate layer fluids' constant viscosities, one can get significant improvement in stability over the pure Saffman-Taylor case. But using the new results given above, we can now a priori decide on various parameter values to home in not only more stabilized system but also shortest unstable band k_{cr}. This is what we show next.

As we have seen above, for the shortest unstable bandwidth k_{cr} one can calculate $\mu_{cr}^{(i)}, i = 1, ..., N$ from μ_r, μ_l, and T_{total} regardless of the number of interfaces and their interfacial tensions $T_i, i = 0, ..., N$ so long as these add up to T_{total}. But how does one select $T_i, i = 1, ... N$, and L to design most stable (least unstable) multi-layer system ? Consider the simplest case when all interfacial tensions are same, say $T_0 = T_1 = ... = T_N$ for a given T_{total} from which all $\mu_{cr}^{(i)}, i = 1, ..., N$ are computed using formulas (25) for the multi-layer system. We call this set of values for parameters $\{\mu_{cr}^{(i)}, T_i, i = 1, ..., N\}$ as group-1. Figure 5 shows plots of the maximum growth rate σ_{max} for the multi-layer system and the maximum pure Saffman-Taylor growth rate σ_{sm} against T_{total}. For a given T_{total}, the value of σ_{sm} is computed using the formula $(2)_1$. It is clear that the growth rates of σ_{max} and σ_{sm} both decrease with increasing T. The general trend shows that σ_{max} is smaller than σ_{sm} for a fixed total interfacial tension T_{total}. But with increasing T, the difference between σ_{max} and σ_{sm} becomes smaller. Nonetheless, we see that the multi-layer Hele-Shaw flows with group-1 values of the parameters used above is less unstable than the corresponding pure Saffman-Taylor case.

According to formulas (25), individual interfacial tension values for given μ_r and μ_l determine the values of $\{\mu_{cr}^{(i)}, i = 1, ..., N\}$. Therefore, choice of these interfacial tension values is most crucial for stabilization under the constraint that T_{total} remains same regardless of the number of interfaces so that all these flows have the same shortest unstable bandwidth k_{cr} (see formula (25)). Although the multi-layer Hele-Shaw flows with group-1 values of the parameters used above is less unstable than the corresponding pure Saffman-Taylor case, it follows from formulas (25) that there exists infinitely many sets of values for $\{T_i, i = 1, ..., N\}$ for the same given T_{total} (=N+1 for the example above) because this total interfacial tension can be unevenly distributed in infinite ways among $N + 1$ interfaces. Equi-distribution of T_{total} among $N + 1$ interfaces as in the previous example may not be the best for stabilization. There may be other better choices of $\{T_i, i = 1, ..., N\}$ for same given T_{total}.

6   Universality Continued

Below, using intuition and heuristic reasoning we show another way to choose the set $\{T_i, i = 1, ..., N\}$ for some given T_{total} that has no influence on the choice of $\{\mu_{cr}^{(i)}, i = 1, ..., N\}$ unlike the previous case (see formulas (25)) and results in more stable system with shortest unstable bandwidth k_{cr}. We know that when $L \to \infty$, individual interfacial instabilities should be independent of each other. Therefore, all $(N + 1)$ dispersion curves $\sigma_i(k), i = 0, ..., N$ for the multi-layer system should approach $(N + 1)$ pure
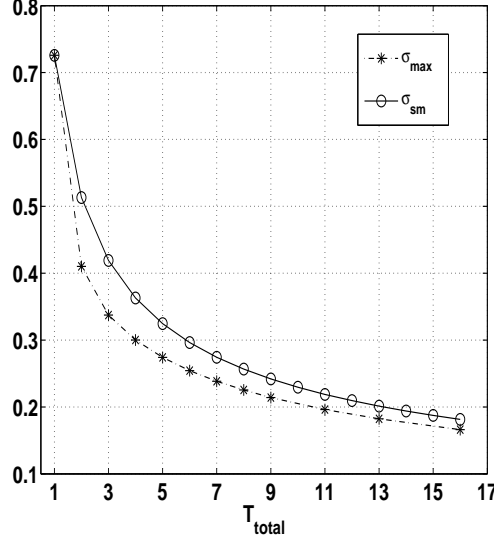
Figure 5: The maximum growth rate σ_{max} for multi-layer flows with group-1 parameters and the maximum growth rate for Saffman-Taylor σ_{sm} versus the interfacial tension T. All the parameter values as $\mu_l = 2$, $\mu_r = 10$, $T_i = 1$ ($i = 0, ...N$), $U = 1$, and $L = 1$.

Saffman-Taylor dispersion curves, one corresponding to each individual interface, when $L \to \infty$. In this limit, maximum growth rate of the multi-layer system, namely $\sigma_{\max} = \max_i\{\max_k \sigma_i(k)\}$, can be described by the pure Saffman-Taylor problem, which is

$$\sigma_{\mathrm{sm,max}} = \max_i\{\sigma_{sm}^{(i)}\}, \tag{29}$$

where $\sigma_{sm}^{(i)} = \max_k \sigma_{st}^{(i)}(k)$ is the maximum Saffman-Taylor growth rate of the $i-$th interface. The problem is to find an optimal group of $\mu_{cr}^{(i)}$ and T_i that minimize the maximum growth rate $\sigma_{\max}$ of multi-layer system. However, this minimization problem is approximately equivalent to minimizing the $\sigma_{\mathrm{sm,max}}$ defined above by (29) because the maximum growth rate of the multi-layer system decreases exponentially with L (see Daripa [4]). Therefore, the problem now is to find the values of $\{\mu_{cr}^{(i)}, i = 1, ..., N\}$ and $\{T_i, i = 1, ..., N+1\}$ that will minimize the maximum of $\{\sigma_{sm}^{(i)}, i = 1, ..., N+1\}$. The solution of this problem becomes easier if all $\{\sigma_{sm}^{(i)}, i = 1, ..., N+1\}$ are taken equal. Even though this heuristic reasoning is not exactly a proof, we will see later that results obtained from this hypothesis provide remarkable gain in stabilization compared to group-1. In fact, we can do better than this. we can find $\mu_{cr}^{(i)}$ and T_i such that all individual interfacial dispersion curves $\sigma_{st}^{(i)}(k)$, $i = 1, \cdots, N$ are identical. Then naturally all $\{\sigma_{sm}^{(i)}, i = 1, ..., N+1\}$ will be equal. Thus, next we select $\mu_{cr}^{(i)}, i = 1, ..., N$ and $T_i, i = 1, ..., N$ that satisfy the following equations so that all $\sigma_{st}^{(i)}(k)$, $i = 1, \cdots, N$ are equal (see formula (1) for $\sigma_{st}(k)$).

$$\frac{Uk(\mu_r - \mu_1)}{\mu_r + \mu_1} = \frac{Uk(\mu_1 - \mu_2)}{\mu_1 + \mu_2} = ... = \frac{Uk(\mu_N - \mu_l)}{\mu_N + \mu_l} \tag{30}$$

and

$$\frac{T_0 k^3}{\mu_r + \mu_1} = \frac{T_1 k^3}{\mu_1 + \mu_2} = ... = \frac{T_N k^3}{\mu_N + \mu_l}, \tag{31}$$

13

so that

$$\sigma_{st}^{(0)}(k) = \sigma_{st}^{(1)}(k) = \ldots = \sigma_{st}^{(N)}(k), \tag{32}$$

for all k. Therefore, zeros k_i of all dispersion curves $\sigma_{st}^{(i)}, i = 0, \ldots, N$ are same, i.e.,

$$k_0 = \ldots = k_N = \sqrt{\frac{U}{T_{\text{total}}}(\mu_r - \mu_l)} \equiv k_{cr}. \tag{33}$$

By solving for $\mu_{cr}^{(i)}$ and T_i from equations (30) and (31), we get a new group of viscosities and interfacial tensions for the shortest width of the unstable band. We call this group-2 parameters.

$$\left. \begin{array}{l} \mu_{cr}^{(1)} = \mu_r^{\frac{N}{N+1}} \mu_l^{\frac{1}{N+1}}, \\ \mu_{cr}^{(2)} = \mu_r^{\frac{N-1}{N+1}} \mu_l^{\frac{2}{N+1}}, \\ \ldots\ldots \\ \mu_{cr}^{(N)} = \mu_r^{\frac{1}{N+1}} \mu_l^{\frac{N}{N+1}}, \\ T_0 = \dfrac{(\mu_r + \mu_{cr}^{(1)})}{\mu_r + \mu_l + 2(\mu_{cr}^{(1)} + \cdots + \mu_{cr}^{(N)})} T_{\text{total}}, \\ T_1 = \dfrac{(\mu_1 + \mu_{cr}^{(2)})}{\mu_r + \mu_l + 2(\mu_{cr}^{(1)} + \cdots + \mu_{cr}^{(N)})} T_{\text{total}}, \\ \ldots\ldots \\ T_N = \dfrac{(\mu_{cr}^{(N)} + \mu_l)}{\mu_r + \mu_l + 2(\mu_{cr}^{(1)} + \cdots + \mu_{cr}^{(N)})} T_{\text{total}}, \end{array} \right\} \tag{34}$$

where $T_{\text{total}} = (T_0 + T_1 + \cdots + T_N)$. Note that notations for the viscosities of all internal layer fluids computed with group-1 formula (25) are same as those computed with group-2 formula (34). However, this should not cause any problem below as these are always referred by their respective groups. Notice that for the three-layer case ($N = 1$), the above formulas yield the group-2 critical viscosity of the fluid in the middle layer as $\mu_{cr}^{(1)} = \sqrt{\mu_r \mu_l}$ and the interfacial tensions $T_0 = \sqrt{\frac{\mu_r}{\mu_r + \mu_l}} T_{\text{total}}$, and $T_1 = \sqrt{\frac{\mu_l}{\mu_r + \mu_l}} T_{\text{total}}$. It is easy to verify that the cut-off wavenumbers k_1 and k_2 of both the modes in this case are k_{cr} given by (33). Interestingly, notice from the formulas above that the viscosities of the fluid layers in succession from left to right in the direction of displacement form a geometric series with geometric ratio $(\mu_r/\mu_l)^{1/(N+1)}$.

7   Numerical Results Continued

For given values of T_{total}, μ_r and μ_l, values of the group-2 parameters $\mu_{cr}^{(i)}$ and T_i are calculated using the above formula (34). Using these interfacial tensions $T_i, i = 0, \cdots, N$, viscosities $\mu_{cr}^{(i)}, i = 1, \cdots, N$ of the interior layer fluids, and given values of U and L, eigenvalues $\sigma^{(i)}(k)$ are numerically computed (see section 3). Figures 6 and 7 show the plots of dispersion curves $\sigma^{(i)}(k)$ versus wave number k for three-, four- and five-layer Hele-Shaw flows when $L = 1$ and $L = 5$ respectively with $T_{\text{total}} = 2, U = 1, \mu_r = 10$, and $\mu_l = 2$ fixed. It is clear that when L increases, all dispersion curves for the multi-layer system come closer to each other. Furthermore, the shortest bandwidth k_{cr} are all equal to 2 as predicted by (33).

In what follows, we compare the effect of the two groups of parameters for $\mu_{cr}^{(i)}$ and T_i, one computed from (25) and the other from (34). Figure 8 shows plots of $\sigma_{\max}$ versus L in cases of three-layer, four-layer and five-layer for both the groups of parameters. Plots in both panels show that flow becomes more stable with increasing number of layers with all other parameter values fixed. We see, as expected, the effect of L
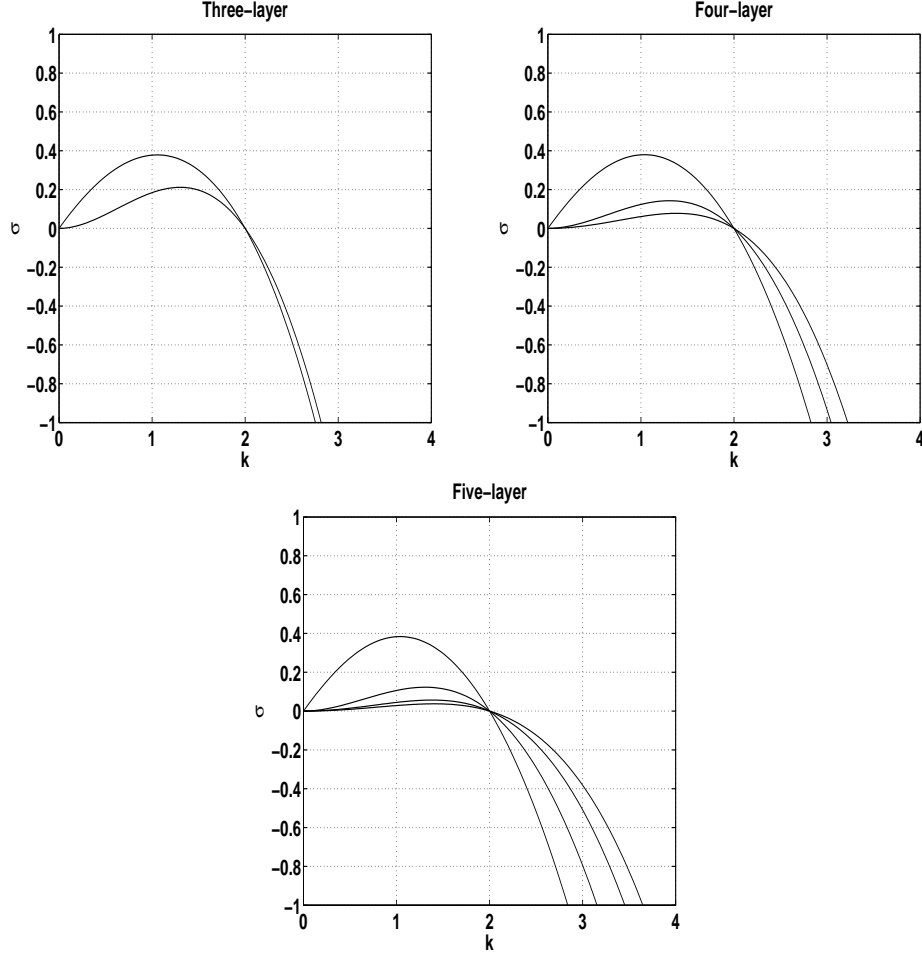
14

Figure 6: Dispersion curves for (25) when $L = 1$: Growth rates σ versus wave number k for three-layer, four-layer and five-layer cases. For three-layer: $\mu = (2, 4.472, 10)$, $T = (1.382, 0.618)$; four-layer: $\mu = (2, 3.42, 5.848, 10)$, $T = (1.038, 0.607, 0.355)$; five-layer: $\mu = (2, 2.9907, 4.472, 6.6874, 10)$, $T = (0.8281, 0.5538, 0.3704, 0.2477)$. All the other parameters are: $\mu_l = 2$, $\mu_r = 10$, $T_{\text{total}} = 2$, $U = 1$ and $L = 1$.
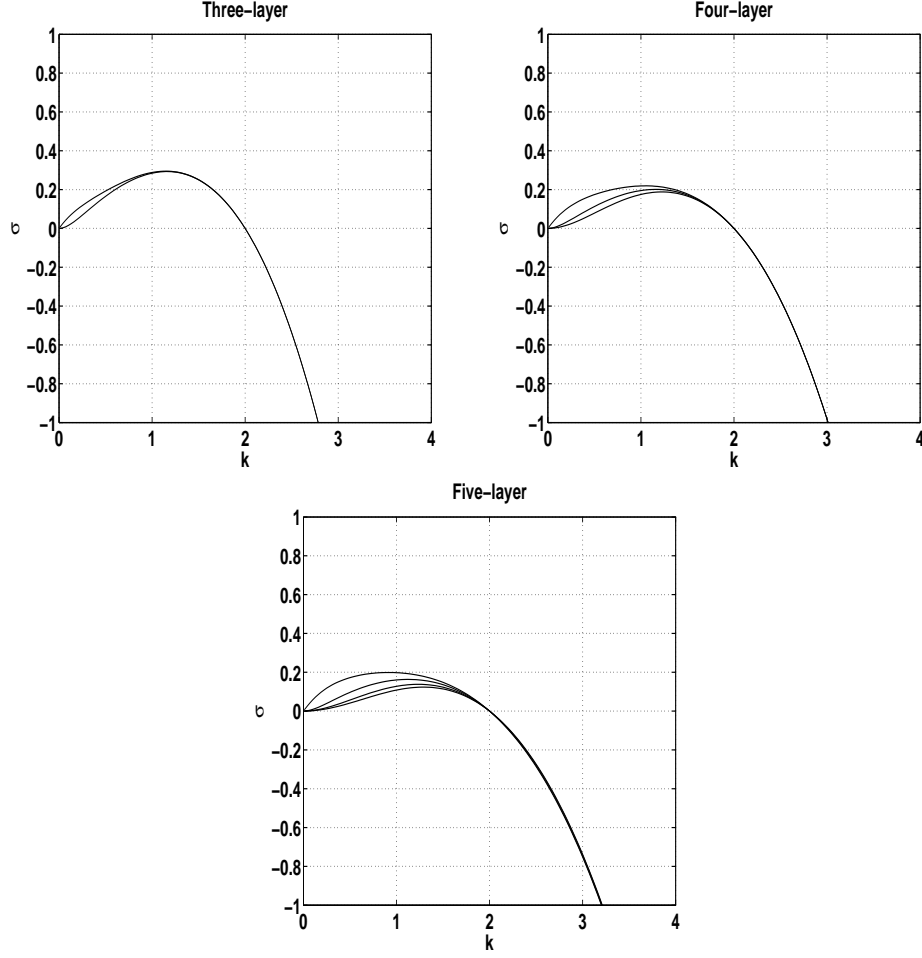
Figure 7: Dispersion curves for (25) when $L = 5$: Growth rates σ versus wave number k for three-layer, four-layer and five-layer cases. For three-layer: $\mu = (2, 4.472, 10)$, $T = (1.382, 0.618)$; four-layer: $\mu = (2, 3.42, 5.848, 10)$, $T = (1.038, 0.607, 0.355)$; five-layer: $\mu = (2, 2.9907, 4.472, 6.6874, 10)$, $T = (0.8281, 0.5538, 0.3704, 0.2477)$. All the other parameters are: $\mu_l = 2$, $\mu_r = 10$, $T_{\text{total}} = 2$, $U = 1$ and $L = 5$.

quickly saturates with both groups of parameters. Notice the significantly improved stabilization capacity of the set of values corresponding to group-2 parameters (right panel) compared to that for the set of group-1 parameters used for plots in the left panel of Fig. 8. Towards this end, we mention that for given T_{total}, μ_r and μ_l, there is only one set of values for group-2 parameters as opposed to infinitely many set of values for the group-1 parameters because of free variables T_i subject to the condition that all these interfacial tensions must add up to given T_{total}. Some of these sets of values from group-1 can even make the system more unstable but many of these sets will also stabilize the system. The choice of the set used for the plots in the left panel of the Fig. 8 is a typical case. Many experiments with various other choices of the set from this group-1 with T_{total}, μ_r and μ_l fixed at the values mentioned in the figure caption of Fig. 8 show that their stabilization capacities do not exceed the one shown in the right panel of Fig. 8 with group-2 parameters' values.
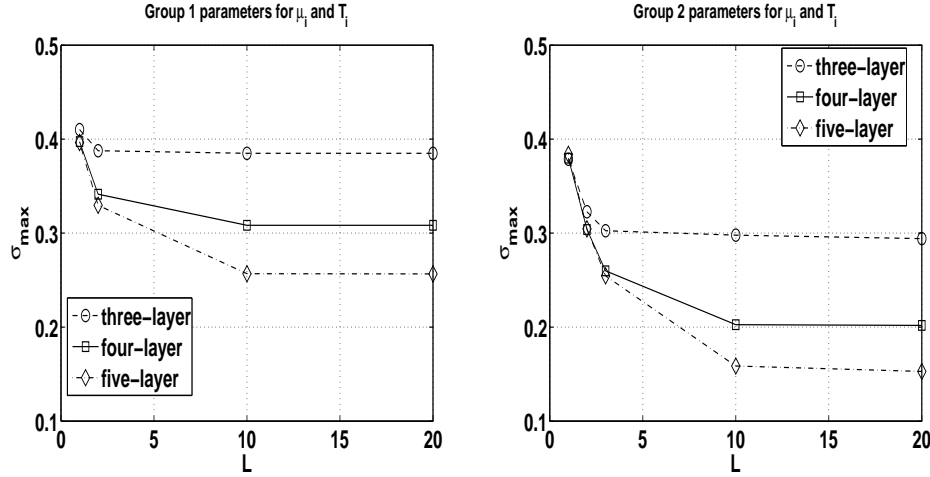

Figure 8: Comparison of Stabilization capacity of two groups (25) and (34) for the same T_{total}, U and L: Plots of the maximal growth rate for σ_{max} versus L for three-layer, four-layer and five-layer cases. The parameters for the left plot are three-layer: $\mu = (2, 6, 10)$, $T_0 = T_1 = 1$; four-layer: $\mu = (2, 4.67, 7.34, 10)$, $T_0 = T_1 = T_2 = 2/3$; five-layer: $\mu = (2, 4, 6, 8, 10)$, $T_0 = T_1 = T_2 = T_3 = 1/2$. For the right plot three-layer: $\mu = (2, 4.472, 10)$, $T = (1.382, 0.618)$; four-layer: $\mu = (2, 3.42, 5.848, 10)$, $T = (1.038, 0.607, 0.355)$; five-layer: $\mu = (2, 2.9907, 4.472, 6.6874, 10)$, $T = (0.8281, 0.5538, 0.3704, 0.2477)$. All the other parameters are: $\mu_l = 2$, $\mu_r = 10$, $U = 1$ and $T_{\text{totoal}} = 2$.

In closing this section, we mention that we have shown the universality of the formulas such as (5) and (6) for k_i, critical viscosity and critical wavenumber. In fact, we have discovered another group (34) of critical viscosities for the same critical wavenmber $(6)_2$. It is worth pointing out that the formula such as (2) for the maximum growth rate and the most dangerous wavenumber for the pure Saffman-Taylor case has no universality appeal for the multi-layer case. The only universality related to the growth rate is a generic pattern of the formula for the upper bound which can be found in Daripa [3] (see formulas (99), (103) and (105) there). In the special case of three-layer (N=1), these formulas for the upper bound reduces to (4).

8 Conclusions

In this paper, we have obtained linear stability results that are universal for multi-layer Hele-Shaw flows in the sense that the results hold for flows involving arbitrary number of interfaces. To summarize, we list the universal stability results below.

1. The cut-off wavenumbers k_i, $i = 0, 1, \cdots, N$ given by (18) are universal meaning that they hold for flows with any number of interfaces. Notice two important facts about this: (i) cut-off wavenumbers are pure Saffman-Taylor cut-off wavenumbers for individual interfaces; (ii) these cut-off wavenumbers do not depend on the length, L, of the middle layer. These properties are universal as well.

2. The unstable bandwidth $k_{\max}$ given by $(19)_1$ is universal as well and it does not depend on L. The shorter bandwidth $k_{\min}$ given by $(19)_2$ which contains unstable waves having both modes (σ_+, σ_-) positive is also universal. These bandwidths also do not depend on L.

3. The critical values of $\mu_{\mathrm{cr}}^{(i)}$ and k_{cr} given by formulas (25) for group-1 and by formulas (34) for group-2 are universal as well and do not depend on L. Since individual growth rates of all interfaces are given by the Saffman-Taylor formulae in the limit $L \to \infty$, one can easily verify that individual Saffman-Taylor growth rates of all interfaces are zero at $k = k_{\mathrm{cr}}$ provided viscosities of the fluids in the N interior layers are $\mu_{\mathrm{cr}}^{(i)}, i = 1, \cdots, N$ (either from group-1 or group-2) and in the case of group-2, the interfacial tensions are T_i from formulas (34).

These results should be useful for stabilization and understanding of flow features in unstable multi-layer Hele-Shaw flows. Application of these new results to stabilization of multi-layer Hele-Shaw flows has been demonstrated in this paper.

References

[1] P. CORLAY AND E. DELAMAIDE, *Evaluation and future of polymer injection in the daqing field*, Revue de l institut francais du petrole, 50 (1995), pp. 237–247.

[2] H. DARCY, *Les fontaines publiques de la ville de Dijon*, Paris, (1856).

[3] P. DARIPA, *Hydrodynamic stability of multi-layer hele-shaw flows*, Journal of Statistical Mechanics, 12 (2008), p. 28.

[4] ——, *Studies on stability in three-layer hele-shaw flows*, Phys. Fluids., 20 (2008), p. Article No. 112101.

[5] P. DARIPA, J. GLIMM, B. LINDQUIST, AND O. MCBRYAN, *Polymer floods: A case study of nonlinear wave analysis and of instability control in tertiary oil recovery*, SIAM J. Appl. Math., 48 (1988), pp. 353–373.

[6] P. DARIPA AND G. PASA, *New bounds for stabilizing hele-shaw flows*, Appl. Math. Lett., 18 (2005), pp. 1293–1303.

[7] ——, *On the growth rate for three-layer hele-shaw flows: Variable and constant viscosity cases*, Int. J. Engg. Sci, 43 (2005), pp. 877–884.

[8] W. Demin, C. Jiecheng, W. Junzheng, Y. Zhenyu, and L. Hongfu, *Summary of asp pilots in daqing oil field*, Paper SPE 57288, (1999).

[9] T. Doscher and F. Wise, *Enhanced crude-oil recovery potential: estimate*, Journal of Petroleum Technology, 28 (1976), pp. 575–585.

[10] P. G. Drazin and W. H. Reid, *Hydrodynamic Stability*, Cambridge Univ. Press., 1981.

[11] Z. J. Fathi and W. Ramirez, *Optimal injection policies for enhanced oil recovery: Part 2surfactant flooding*, Paper SPE 12814, (1982).

[12] F. Fayers, ed., *Enhanced Oil Recovery*, Elsevier, The Netherlands, 1981.

[13] S. B. Gorell and G. Homsy, *A theory of the optimal policy of oil recovery by the secondary displacement process*, SIAM J. Appl. Math., 43 (1983), pp. 79–98.

[14] H. S. HeleShaw, *On the motion of a viscous fluid between two parallel plates*, Trans R. Inst. Na. Archit. Lond., 40 (1898), pp. 18–.

[15] L. W. Lake, *Enhanced Oil Recovery*, Prentice Hall, Englewood Cliffs, N.J., 1989.

[16] W. Littman, *Polymer Flooding: Developments in Petroleum Science*, Elsevier, Amsterdam, 1998.

[17] N. Mungan, *Improved waterflooding through mobility control*, Canad. J. Chem. Engng., 49 (1974), pp. 32–37.

[18] R. Needham and P. Doe, *Polymer flooding review*, Journal of Petroleum Technology, 12 (1987), pp. 1503–1507.

[19] J. Pearson, *The stability of some variable viscosity flows with application to oil extraction*, unpublished, Cambridge Univ., (1977).

[20] G. Pope, *The application of fractional flow theory to enahcned oil-recovery*, Society of petroleum engineers journal, 20 (1980), pp. 191–205.

[21] G. Pope and W. Wade, *Lessons from enhanced oil recovery research for surfactant enhanced aquifer remediation*, in Surfactant-Enhanced Remediation of Subsurface Contamination, 1995.

[22] G. A. Pope and R. C. Nelson, *A chemical flooding compositional simulator*, Soc. Pet. Eng. J., 18(5) (1978), pp. 339–354.

[23] P. Saffman and G. Taylor, *The penetration of a fluid into a porous medium or Hele-Shaw cell containing a more viscous liquid*, Proceedings of the Royal Society of London, Series A, 245 (1958), pp. 312–329.

[24] D. Shah and R. Schecter, eds., *Improved Oil Recovery by Surfactants and Polymer Flooding*, Academic Press, New York, NY, 1977.

[25] R. L. Slobod and J. S. Lestz, *Use of a graded viscosity zone to reduce fingering in miscible phase displacements*, Producers Monthly, 24 (1960), pp. 12–19.

[26] K. Sorbie, *Polymer-Improved Oil Recovery*, CRC Press, Boca Raton, Florida, 1991.

[27] K. Taylor and H. Nasr-El-Din, *Water-soluble hydrophobically associating polymers for improved oil recovery: A literature review*, Journal of Petroleum Science and Engineering, 19 (1998), pp. 265–280.

[28] A. Uzoigwe, F. Scanlon, and R. Jewett, *Improvement in polymer flooding: The programmed slug and the polymer-conserving agent*, J. Petrol. Tech., 26 (1974), pp. 33–41.

[29] J. Vargo, J. Turner, B. Vergnani, M. Pitts, K. Wyatt, H. Surkalo, and D. Patterson, *Alkaline-surfactant/polymer flooding of the cambridge field*, Paper SPE 55663, (1999).

[30] L. Zerpaa, N. Queipoa, T. S. Pintosa, and J. Salagerb, *An optimization methodology of alkaline-surfactant-polymer flooding processes using field scale numerical simulation and multiple surrogates*, Journal of Petroleum Science and Engineering, 47 (2005), pp. 197–208.

[31] Q. Zhijian, Z. Yigen, Z. Xiansong, and D. Jialin, *A successful asp flooding in gudong oil field*, Paper SPE 39613, (1999).

[32] Z. Zhijun and H. Yongmei, *Economic evaluation shows polymer flooding effectiveness*, Oil & Gas Journal, 21 (2002), pp. 56–59.